Mukt Shabd Journal ISSN NO : 2347-3150

MIXED CONVECTIVE HEAT TRANSFER FLOW OF NANOFLUID IN CYLINDRICAL ANNULUS WITH VARIABLE VISCOSITY, ELECTRICALLY CONDUCTIVITY AND ACTIVATION ENERGY

Dr. D. Chitti Babu
Principal, Govt. Degree College, Seethanagaram, East Godavari(Dt.),A.P., India
Mobile : +91 7659854317, Email: chittibabu.d9@gmail.com

Abstract: The influence of activation energy, variable viscosity and electrical conductivity on MHD mixed convective heat and mass transfer flow of nanofluid through a porous medium in a Co-axial cylindrical duct. The governing equations have been solved by using numerical techniques. The velocity, temperature and nanoconcentration have been demonstrated at different axial positions. The Nusselt and Sherwood numbers are evaluated for different parametric variations. Increase in viscosity parameter(B)/variable electrical conductivity with nanoconcentration (β1)enhances velocity, temperature and reduces nanoconcentration. Nusselt number(Nu) reduces with electrical conductivity with temperature (α1) on both the cylinders.

Key Words : Activation Energy, Variable viscosity and electrical conductivity, Brownian motion, Thermophoresis, thermal radiation, Cylindrical annulus.

1. INTRODUCTION:

The concept of nanofluid has been introduced by Choi [6]. He has given clear description about the heat transfer characteristics of nanofluids. Natural convection of Al_2O_3-water and CuO-water nanofluid inside a cylindrical enclosure heat from one side and cooled from the other side was studied by Putra et al., [22]. They found that the natural convection heat transfer coefficient was lower than that of pure water. Wen and Ding [37] investigated the natural convection of TiO_2-water in a vessel composed of two discs. Their results showed that the natural convection decreases by increasing the volume fraction of nanoparticle. Several authors (Mokhtari Moghari et al. [19], Parvin et al. [21], Soleimani et al. [28], Abu-Nada et al. [1], Abu-Nada [2], Sree Devi et al. [29], Nagasasikala et al. [20], Sudarsana Reddy et al., [32], Madhusudhana Reddy et al., [16], Sulochana and Ramakrishna [33], Shivakumara et al. [26], Mallikarjuna et al.[18] and Alivene et al., [3]) have been investigated two phase mixed convection Al_2O_3-water nanofluid flow in an annulus. Sudhakara Reddy [31] has analysed the effect of magnetic field on convective heat and mass transfer flow nanofluid in a cylindrical annulus in the presence of non-uniform heat sources. Ramakrishna and Prasada Rao [23] have investigated convective heat and mass transfer flow of Cuo-water and Al_2O_3-Water nanofluid in cylindrical annulus in the presence of heat sources.

Convection flow in nature and engineering phenomena requires that viscosity and thermal conductivity of fluids vary with temperature. Dulal and Hiramony [8] analysed the effects of temperature-dependent viscosity and variable thermal conductivity on mixed convective diffusion flow. They found that velocity profile increases while temperature decreases with increase in mixed convection. Vajravelu et al [36], Singh and Shweta [27] and Isaac and Anselm [12] shoed that, velocity distribution decreases with increase in viscosity while the temperature profiles increase with increase in variable viscosity. Devi and Prakash [7] examined temperature-dependent viscosity and thermal conductivity effects on hydromagnetic flow over a slandering stretching sheet. They concluded that, increase in viscosity decreases the velocity profiles. The work of Animasaun [4] concluded that the fluid velocity decreases while temperature increases with increasing viscosity. The works of Gopal

et al [10]. Makinde et al. [17] they have shown that the velocity profiles decrease with increasing viscosity while temperature profiles decrease with increase in viscosity.

Several authors have been evaluated to effect of Arrhenius activation energy and dual stratifications on the MHD flow of a Maxwell nanofluid with various heating (Sandhya et al. [25], Zeeshan et al. [38], Saida Rashid et al. [24], Gireesha et al. [9]). Khan et al [15], Ijaj Khan et al [11], made brief discussion on Activation Energy impact in Nonlinear Radiative Stagnation Point Flow of Cross Nanofluid and also analysed the Arrhenius activation energy impact in binary chemically reactive flow of TiO_2-Cu-H_2O hybrid nanomaterial.

In this paper, the effect of variable electrical conductivity, viscosity, activation energy, Brownian motion, thermophoresis on MHD free and forced convective heat and mass transfer flow through a porous medium in a Co-axial cylindrical duct where the boundaries are maintained at uniform temperature and nanoconcentrations. The non-linear coupled equations have been solved by using Finite element analysis with quadratic polynomials as approximations functions.

2. FORMULATION OF THE PROBLEM:

We consider the free and forced convection flow of a nanofluid in a vertical circular annulus through a porous medium whose walls are maintained at a uniform heat and concentration. The Brinkman-Forchhimer-Extended Darcy model which accounts for the inertia and boundary effects has been used for the momentum equation in the porous region. The momentum, energy and diffusion equations are coupled and non-linear. Also the flow is unidirectional along the axial direction of the cylindrical annulus. The nanofluid dynamic viscosity is assumed to be an exponential decreasing function of temperature given by

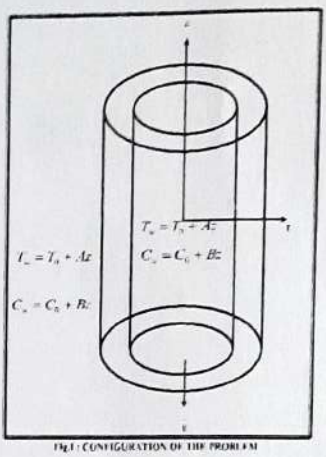

Fig.1: CONFIGURATION OF THE PROBLEM

$$\mu_f(T) = \mu_o Exp(-\beta(T - T_o)) \tag{1}$$

where μ_o is dynamic viscosity β is the

Making use of Boussinesq and Rosseland approximation the governing equations under radial magnetic field

$$0 = -\frac{\partial p}{\partial z} + \mu_o e^{-\beta(T-T_o)}\left(\frac{\partial^2 u}{\partial r^2} + \frac{1}{r}\frac{\partial u}{\partial r}\right) - (\mu_o \beta(T_w - T_o))e^{-\beta(T-T_w)}\frac{\partial u}{\partial r}\frac{\partial T}{\partial r} - \frac{\mu_0 e^{-\beta(T-T_o)}}{k_p}u -$$
$$- \frac{\sigma(T,C)\mu_e^2 H_o^2}{\rho_f}\left(\frac{u}{r^2}\right) + (1-C_o)\rho_f \beta_T g[(T-T_0) - \frac{(\rho_p - \rho_{f_o})\beta_C}{(1-C_o)\rho_f \beta_T}(C - C_0)] \tag{3}$$

$$(\rho C_p)u\frac{\partial T}{\partial z} = k_f\left(1 + \frac{16\sigma^* T_o^3}{3\beta_R k_f}\right)\left(\frac{\partial^2 T}{\partial r^2} + \frac{1}{r}\frac{\partial T}{\partial r}\right) + Q_1'(C - C_o) +$$
$$+ \tau\left(D_B \frac{\partial T}{\partial r}\frac{\partial C}{\partial r} + \left(\frac{D_T}{3T_0}\right)\left(\frac{\partial T}{\partial r}\right)^2 + 2\mu_f(T)\left(\frac{\partial u}{\partial r}\right)^2 + \sigma\mu_e^2 H_o^2(u^2)\right) \tag{4}$$

$$u\frac{\partial C}{\partial z} = D_B\left(\frac{\partial^2 C}{\partial r^2} + \frac{1}{r}\frac{\partial C}{\partial r}\right) - k_c\left(\frac{T}{T_0}\right)^2 Exp\left(-\frac{E_a}{kT}\right)(C - C_o)$$

where u is the axial velocity in the porous region, T , C are the temperature and nanoconcentration of the fluid, k_p is the permeability of porous medium, k_f is the thermal diffusivity, D_B is the Brownian motion diffusion coefficient, D_T is the thermophoresis diffusion coefficient, K_T mass diffusion ratio, βc is the coefficient of the thermal expansion,

ISSN NO : 2347-3150

q_R is the radiation absorption coefficient,Cp is the specific heat, ρ is density ,g is gravity, ρ_f is the effective density, $\mu_f(T)$ is the effective dynamic viscosity, k_f is the thermal conductivity coefficient of the nanofluid, σ^* is the Stefan-Boltzman constant, β_R is the mean absorption constant. The relevant boundary conditions are

u=0, T=Ti , C=Ci at r = a
u=0, T=To , C=Co at r = b (5)

The variable electrical conductivity $\sigma(T,C)$ is defined [Ref.2a]as

$$\sigma(T,C) = \sigma_o[1+\alpha_1(\frac{T-T_o}{T_i-T_o})+\beta_1(\frac{C-C_o}{C_i-C_o})],$$

where σ_o is the constant electrical conductivity, α_1 is the temperature dependent electrical conductivity parameter and β_1 is the nanoparticle concentration dependent electrical conductivity parameter.

The axial temperature and nanoconcentration gradients $\frac{dT}{dz}$ and $\frac{dC}{dz}$ are assumed to be constant, say A and B.

Introducing non-dimensional variables

$$z^* = \frac{z}{a} \quad , \quad \eta = \frac{r}{a} \quad , \quad u^* = (\frac{a}{\nu})u \qquad p^* = \frac{pa\delta}{\rho\nu^2} ,$$

$$\theta^*(r^*) = \frac{T^*-T_0}{(T_i-T_0)} \quad , \quad C^*(r^*) = \frac{C^*-C_0}{(C_i-C_0)} \quad , \quad s = \frac{b}{a}, P_1 = \pi = \frac{dp}{dz} \tag{6}$$

Introducing these non-dimensional variables, the governing equations in the non-dimensional form are (on removing the stars)

$$0 = (\frac{\partial^2 u}{\partial r^2}+\frac{1}{r}\frac{\partial u}{\partial r}) - B\,(\frac{d\theta}{dr})(\frac{du}{dr}) + (K)u + (e^{B\theta})[\pi + \varepsilon\frac{M^2(\pi+\alpha_1\theta+\beta_1\phi)}{r^2})u - \\ -G(\theta+Nr\phi)] \tag{7}$$

$$(1+\frac{4Rd}{3})(\frac{\partial^2\theta}{\partial r^2}+\frac{1}{r}\frac{\partial\theta}{\partial r}) + Q_1 C + Nb(\frac{\partial\theta}{\partial r})(\frac{\partial C}{\partial r}) + Nt(\frac{\partial\theta}{\partial r})^2 - \\ -\Pr(N_T)u + Ec(e^{-B\theta})\Pr(\frac{\partial u}{\partial r})^2 + EcM^2\Pr(u^2) = 0 \tag{8}$$

$$(\frac{\partial^2 C}{\partial r^2}+\frac{1}{r}\frac{\partial C}{\partial r}) - \gamma(1+\delta\theta)(C)Exp(-\frac{E_1}{(1+\delta\theta)}) + (\frac{Nt}{Nb})\left(\frac{\partial^2\theta}{\partial r^2}+\frac{1}{r}\frac{\partial\theta}{\partial r}\right) - Sc(Nc)u = 0 \tag{9}$$

where

$G = \frac{\beta_T Aa(1-C_o)ga^3}{\nu^2}$ (Grashof number), $B = \beta(T_i - T_o)$ (Viscosity parameter)

$\delta = P_1 T_0 Aa$ (Temperature difference parameter), $E1 = \frac{E_n}{kT_0}$ (Activation energy parameter)

$Nr = \frac{(\rho_p-\rho_{f_o})\beta_c B}{(1-C_0)\beta_T A}$ (buoyancy parameter), $M^2 = \frac{\sigma_o\mu_e^2 H_0^2 a^2}{\mu_o}$ (magnetic parameter)

$K = \frac{a^2}{k_p}$ Inverse Darcy parameter), $\Pr = \frac{\mu_0 C_p}{k_f}$ (Prandtl number)

$\alpha_f = \frac{k_f}{(\rho C)_f}$, $Le = \frac{\alpha_f}{D_B}$ (Lewis number), $\gamma = \frac{k_c^2}{D_B}$ (Chemical Reaction parameter),

$Nb = \frac{\tau D_B (C_i - C_o)a}{C_p \alpha_{nf}}$ (Brownian motion parameter), $Nt = \frac{D_{nf} K_T (C_i - C_o)}{C_p (T_i - T_o)\alpha_{nf}}$ (Thermophoresis parameter), $Ec = \frac{v_f}{C_p P \Lambda a^5}$ (Eckert number), $Q_1 = \frac{Q_1'(C_i - C_o)a^2}{C_p(T_i - T_o)}$ is the radiation absorption parameter, $N_T = \frac{Aa}{T_i - T_o}$ is non-dimensional temperature gradient, $N_c = \frac{Ba}{C_i - C_o}$ is the non-dimensional concentration gradient.

The corresponding non-dimensional conditions are

u=0	$\theta = 1$	C=1	at η=1
u=0	$\theta = 0$	C=0	at η=s

3. FINITE ELEMENT ANALYSIS

The finite element analysis with quadratic polynomial approximation functions is carried out along the radial distance across the circular duct. The behavior of the velocity, temperature and nanoconcentration profiles has been discussed computationally for different variations in governing parameters. The Galerkin method has been adopted in the variational formulation in each element to obtain the global coupled matrices for the velocity, temperature and nanoconcentration in course of the finite element analysis.

Choose an arbitrary element e_k and let u^k, θ^k and C^k be the values of u, θ and C in the element e_k.

We define the error residuals as

$$E_p^k = \frac{d}{dr}\left(r\frac{du^k}{dr}\right) - B\left(\frac{du^k}{dr}\right)\left(\frac{d\theta^k}{dr}\right) - (K)u + e^{B\theta}(1 + G(\theta^k + Nr\varphi^k) - \left| \right. \quad (10)$$

$$\left. - \frac{M^2(\pi + \alpha_1\theta^k + \beta_1\phi^k)}{r^2}\right) r u^k 1]$$

$$E_\theta^k = \frac{(1 + \frac{4Rd}{3})}{\Pr}\frac{d}{dr}\left(r\frac{d\theta^k}{dr}\right) - r\Pr(N_T)u^k + Nb\left(\frac{d\theta^k}{dr}\right)\left(\frac{d\phi^k}{dr}\right) + \left| \right. \quad (11)$$

$$\left. + Nt\left(\frac{d\theta^k}{dr}\right)^2 + +2Ec(e^{-B\theta})\left(\frac{du^k}{dr}\right)^2 + EcM^2(u^k)^2 + Q_1\phi^k \right.$$

$$E_c^k = \frac{d}{dr}\left(r\frac{dC^k}{dr}\right) - rLe(N_c)(u^k) - \gamma(1 + n\delta\theta^k)(C^k)Exp\left(-\frac{E_1}{(1 + \delta\theta^k)}\right) + \left| \right. \quad (12)$$

$$\left. + \left(\frac{Nt}{Nb}\right)\frac{d}{dr}\left(r\frac{d\theta^k}{dr}\right)\right.$$

where u^k, θ^k & C^k are values of u, θ& C in the arbitrary element e_k. These are expressed as linear combinations in terms of respective local nodal values.

$$u^k = u_1^k\psi_1^k + u_2^k\psi_1^k + u_3^k\psi_3^k,\ \theta^k = \theta_1^k\psi_1^k + \theta_2^k\psi_2^k + \theta_3^k\psi_3^k,\ C^k = C_1^k\psi_1^k + C_2^k\psi_2^k + C_3^k\psi_3^k$$

where ψ_1^k, ψ_2^k-------- etc are Lagrange's quadratic polynomials.

Galerkin's method is used to convert the partial differential Eqs. (11) – (12) into matrix form of equations which results into 3x3 local stiffness matrices. All these local matrices are assembled in a global matrix by substituting the global nodal values of order I

ISSN NO : 2347-3150

and using inter element continuity and equilibrium conditions. In solving these global matrices an iteration procedure has been adopted to include the boundary and effects in the porous medium. The iteration process is carried out until $/ f_{i+1} - f_i / \leq 10^{-6}$ is achieved.

4.COMPARISON :

In the absence of variable electrical conductivity ($\alpha 1 - 0, \beta 1 - 0$), the results are in good agreement with ***Gayatri***[8a]

Table : 1

Parameter		*Gayatri*[8a]				Present Results			
		Skin Friction (τ)		Nuselt Number		Skin Friction (τ)		Nusselt Number	
		τ(1)	τ(2)	Nu(1)	Nu(2)	τ(1)	τ(2)	Nu(1)	Nu(2)
Rd	1.5	-0.496116	0.496656	-0.327721	0.328012	-0.496009	0.496659	-0.327746	0.328014
	3.5	-0.496132	0.496672	-0.125835	0.125947	-0.49610	0.496677	-0.125831	0.125953
	5.0	-0.496136	0.496726	-0.077223	0.735145	-0.49611	0.496762	-0.077227	0.735162
Ec	0.1	-0.49574	0.496279	-0.543313	0.543851	-0.49575	0.496272	-0.543319	0.543855
	0.2	-0.495634	0.496173	-0.759495	0.760258	-0.495636	0.496171	-0.759501	0.760261
	0.3	-0.495569	0.496109	-0.867466	0.868374	-0.495564	0.496111	-0.867446	0.868378
B	0.2	-0.496116	0.496656	-0.327711	0.328009	-0.496009	0.496721	-0.327714	0.328013
	0.4	-0.496106	0.496566	-0.327721	0.328012	-0.496105	0.496572	-0.327723	0.328009
	0.6	-0.496099	0.496456	-0.327725	0.328015	-0.496101	0.496443	-0.327729	0.328028
Nb	0.1	-0.496112	-0.496109	-0.327715	0.328009	-0.496162	-0.496111	-0.327721	0.328013
	0.2	-0.496116	-0.496116	-0.327721	0.328012	-0.496009	-0.496119	-0.327776	0.328013
	0.3	-0.496118	-0.496122	-0.327724	0.328022	-0.496120	-0.496131	-0.327728	0.328026
Nt	0.1	-0.495823	0.496359	-0.326903	0.327193	-0.495833	0.496346	-0.326914	0.327199
	0.2	-0.495783	0.496322	-0.326839	0.32713	-0.495785	0.496317	-0.326843	0.327128
	0.3	-0.495746	0.496285	-0.326776	0.27066	-0.495749	0.496284	-0.326781	0.270669
El	0.2	-0.495879	0.496419	-0.327005	0.327266	-0.495889	0.496423	-0.327009	0.327271
	0.4	-0.495896	0.496436	-0.327035	0.327325	-0.495902	0.496437	-0.327036	0.327329
	0.6	-0.495897	0.496442	-0.327136	0.327467	-0.495906	0.496444	-0.327136	0.327466

5. SKIN FRICTION, NUSSELT NUMBER AND SHERWOOD NUMBER

The skin friction (τ), rate of heat & mass transfer (Nusselt & Sherwood number) is evaluated using the formula $\tau = (\frac{du}{dr})_{r=1,1+\varepsilon}$, $Nu = -(\frac{d\theta}{dr})_{r=1,1+\varepsilon}$, $Sh = -(\frac{dC}{dr})_{r=1,1+\varepsilon}$

6. RESULTS AND DISCUSSION:

In this analysis we demonstrate the impact of activation energy, variable electrical conductivity, viscosity, Brownian-motion and thermophoresis on hydromagnetic convective heat and mass transfer flow of nanofluid in a circular annulus.The non-linear ,coupled equations governing the flow,heat and mass transfer have been solved by using Runge-Kutta Fourth order method along with shooting technique. The velocity, temperature and nanoconcentration have been analysed for different parametric variations

Figs.2a-2d represent velocity(u), temperature(θ) and nanoconcentration (C) with Grashof numbere(G) and magnetic parameter(M). From the profiles we find that velocity enhances with increase in G and reduces with M, The temperature rises with G and M in the entire flow region.the nanoconcentration(C) reduces with G and enhances with M. This may be due to the fact that the thermal boundary layer becomes thicker with increase in G and M while solutal layer becomes thinner with G and thicker with M.

Figs.3a-3d exhibit u,0,C with viscosity parameter(B) and buoyancy ratio(Nr). The velocity(u) and temperature(θ) experience an enhancement with rising values of viscosity parameter(B) and Nanoconcentration (C) depreciates with B.With respect to buoyancy ratio(Nr) we find that when the molecular buoyancy force dominates over the thermal

buoyancy forces are in the same direction.(figs 3a-3d)

The effect of porous medium(K) and Forchheimer parameter(fs) on u,θ,C can be seen from figs.4a-4d. From the profiles we notice that lesser the porous permeability smaller the velocity ,temperature and larger the nanoconcentration.Higher the Forchheimer parameter(fs) lesser the velocity, temperature and larger the nanoconcentration in the flow region.This may be attributed to the fact that the effect of inertia and boundary effects is to reduce the thickness of the momentum and thermal boundary layers.

The effect of chemical reaction(γ) on u,θ and C can be seen from figs.5a-5d.From the profiles we find that the velocity upsurges in both degenerating and generating chemical reaction cases.The temperature and nanboconcentration depreciate in degenerating chemical reaction case and enhance in the generating case.

Figs.6a-6d show the variation of u,θ,C with thermal radiation(Rd) and radiation absorption(Q1).Higher the radiative heat flux smaller the velocity, temperature and larger the nanocentration in the flow region. An increase in Q1 leads to a growth in momentum and thermal boundary layer thickness, and decay in solutal boundary layer, which in turn rises the velocity,temperature and decays the nanoconcentration in the flow region.

Figs.7a-7d show u, θ and C with activation energy (E1) and temperature difference ratio(δ). From the graphs we find that the velocity decays with E1 and enhances with δ. The temperature and nanoconcentration experience an enhancement with increasing values of E1 and δ.This may be attributed to the fact that increase in activation and tempetrature difference ratio results in growth of the thermal and solutal boundary layers.

Figs.8a-8d exhibit the effect of Brownian motion (Nb) and thermophoresis (Nt) on u,θ and C. An increase in Brownian motion parameter(Nb) reduces the velocity, enhances temperature and nanoconcentration in the flow region while increase in thermophoresis parameter(Nt) leads to rise in growth in momentum and thermal boundary layers and dcecay in solutal boundary layer.

Figs.9a-9d demonstrate velocity, temperature and nanoconcentration with variable electrical conductivity parameters (α1,β1). An increase in variable electrical conductivity(α1) with temperature results in depreciation in velocity, enhancement in temperature, nanoconcentration in the flow. This may be due to the fact that increase in α1 leads to a decay in momentum boundary layer thickness, grows the thickness of the thermal and solutal boundary layers. An augmentation in electrical conductivity with nanoconcentration (β1) leads to thickening of the momentum and thermal boundary layers and thinning of the solutal boundary layer thickness.

Figs.10a-10d demonstrate the variation of flow variables (u,θ,C) with Lewis number (Le) and index number(n).Increase in Lewis number enhances velocity,reduces temperature and nanoconcentration in the flow region.This may be due to the fact that increase in Le leads to a growth in momentum boundary layer and decay in thermal,solutal boundary layers. Also velocity rises, temperature and nanoconcentration decay with agumented values of index number(n).

The skin friction (Cf),rate of heat and mass transfer (Nu,Sh) on the walls r=1,2 of the circular annulus have evaluated for different parametric variations and are presented in table.2. From the tabuler values we find that the skin friction(Cf)enhances on both the cylinders(r=1,2) with rising values of G/M/B/Q1/δ/Nt/Le/n/β1 while it reduces on r=1&2 with increasing values of K/Nr/fs/Rd/E1/Nb/α1.Thus the skin friction on the inner and outer cylinders decay with increase in variable electrical conductivity with temperature and grows with increase in electrical conductivity(β1)with nanoconcentration.An increase in chemical reaction parameter(γ)leads to a rise in skin friction on both the cylinders.

ISSN NO : 2347-3150

The rate of heat transfer(Nu)reduces on the inner cylinder(r=1) and enhances on the outer cylinder(r=2) with rising values of G/M/B/Q1/E1/δ/Nb/Nt while increasing values of K/fs/Nr/Rd/n leads to rise in Nu on the inner cylinder(r=1) and decay in Nu on the outer cylinder(r=2).An increase in Le and α1 ,declines Nu on both the cylinders. In degenerating chemical reaction case(γ>0)Nu enhances on the inner cylinder r=1 and reduces on the outer cylinder r=2.

The rate of mass transfer (Sh) on the inner and outer cylinders(r=1&2) enhances with rising values of G/M/Nt/α1. Sherwood number enhances on the inner cylinder(r=1) and reduces on the outer cylinder(r=2) with augmented values of B/Q1/δ/Le/n/β1.Also Sh reduces on r=1 and enhances on r=2 with increasing values of Nr/K/fs/Rd/E1/Nb. Sh grows on r=1 and decays on r=2 in both degenerating/generating chemical reaction cases.

Thus variable electrical conductivity with temperature (α1)reduces the skin friction, rate of heart transfer,enhances mass transfer on both the cylinders while electrical conductivity with nanoconcentration(β1)increases Cf,Sh ,reduces on r=1 and enhances Cf, Nu, reduces Sh on r=2.

7. CONCLUSIONS:

The equations of momentum,energy and diffusion have been solved by Galerkion Finite element analysis and velocity,temperature and nanoconcentration have been discussed for different parameters.The important findings are:

1) Increase in Grashof number(G)/viscosity parameter(B)/radiation absorption(Q1)/ thermophoresis parameter(Nt)/variable electrical conductivity with nanoconcentration (β1)enhances velocity,temperature and reduces Nanoconcentration.
2) Increase in magnetic parameter(M)/activation energy(E1)/Brownian motion parameter (Nb)/ electrical conductivity with temperature (α1) reduces the velocity, enhances the temperature and nanoconcentration in the flow region.
3) Enhancement in buoyancy ratio(Nr)/porous parameter(K)/Forchheimer parameter(fs)/ radiation parameter(Rd) reduces velocity, temperature and enhances the nanoconcentration in the flow region.
4) Increase in temperature difference ratio(δ)enhances velocity,temperature and nanoconcentration in the entire region..
6) Velocity enhances,temperature and nanoconcentration reduce in degenerating chemical reaction case while in generating chemical reaction case velocity, temperature and nanoconcentration experience enhancement in the flow region.
7) Increase in Grashof number(G)/magnetic parameter(M)enhances skin friction and Sherwood number on both the cylinders.
8) Increase in K/Nr/fs/Rd/E1/Nb/α1 decays skin friction,Nu reduces with Le and electrical conductivity with temperature (α1) on both the cylinders.Sh reduces with Rd on r=1 and enhances on r=2
9) Increase in viscosity parameter(B)enhances Cf,Sh,reduces Nu on r=1and on r=2,Cf,Nu enhances,Sh reduces.
9) Sherwood number(Sh) enhances on the inner cylinder r=1 with α1 and β1 and on r=2,it enhances α1reducres β1,

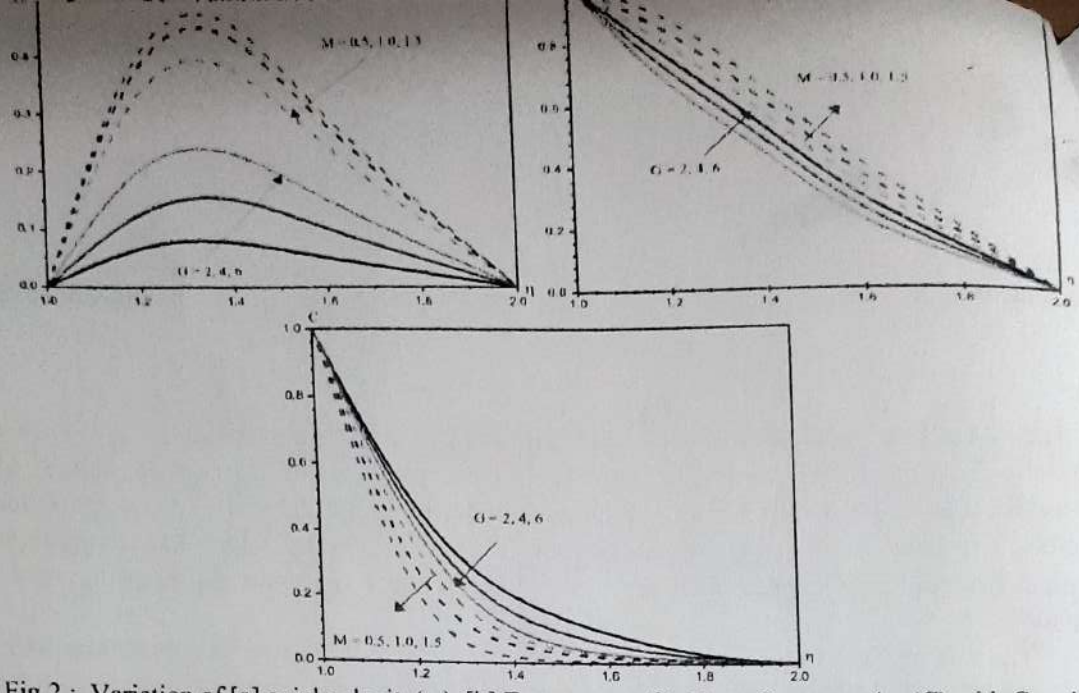

Fig.2 : Variation of [a] axial velocity(w), [b] Temperature(θ), Nano-Concentration(C) with G and M B=0.2, Nr=0.5, K=0.2, fs=0.1, Nb=0.3, Nt=0.1, E1=0.1, δ=0.2, γ=0.5, Rd=0.5, Q1=0.5, α1=0.1, β1=0.2, Le=1, n = 0.5

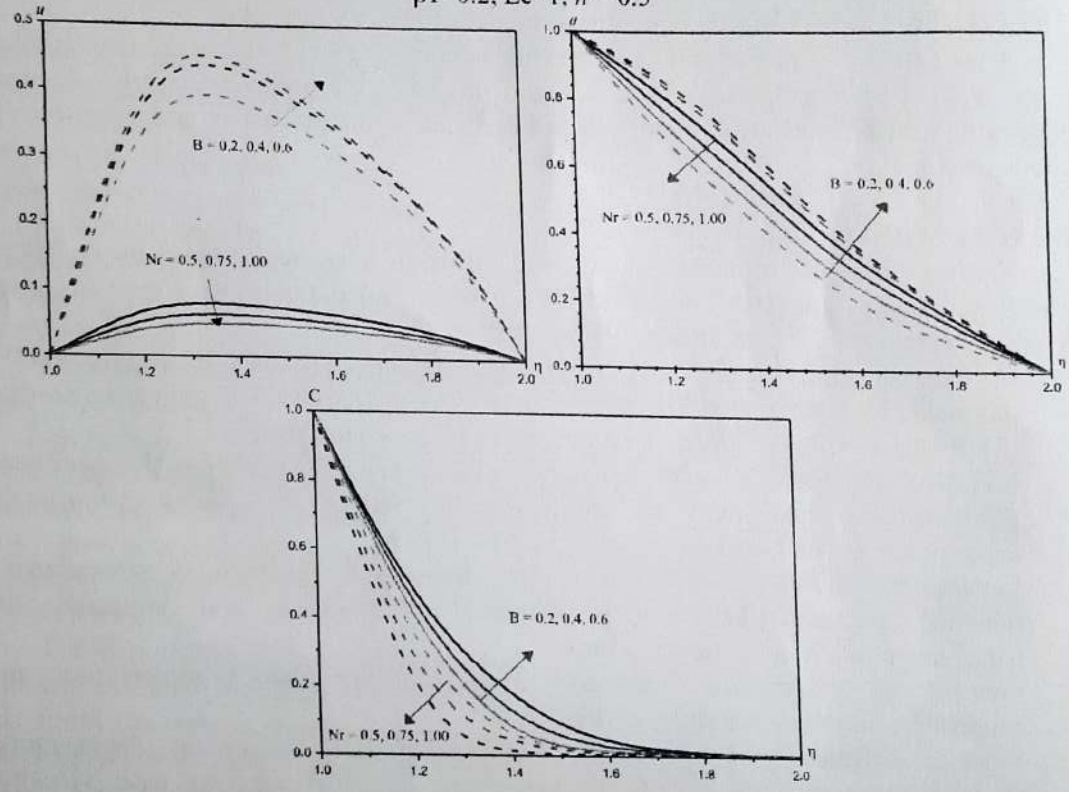

Fig.3 : Variation of [a] axial velocity(w), [b] Temperature(θ),Nano-Concentration(C) with B and Nr G=2, M=0.5, K=0.2, fs=0.1, Nb=0.3, Nt=0.1, E1=0.1, δ=0.2, γ=0.5, Rd=0.5, Q1=0.5, α1=0.1, β1=0.2, Le=1, n = 0.5

ISSN NO : 2347-3150

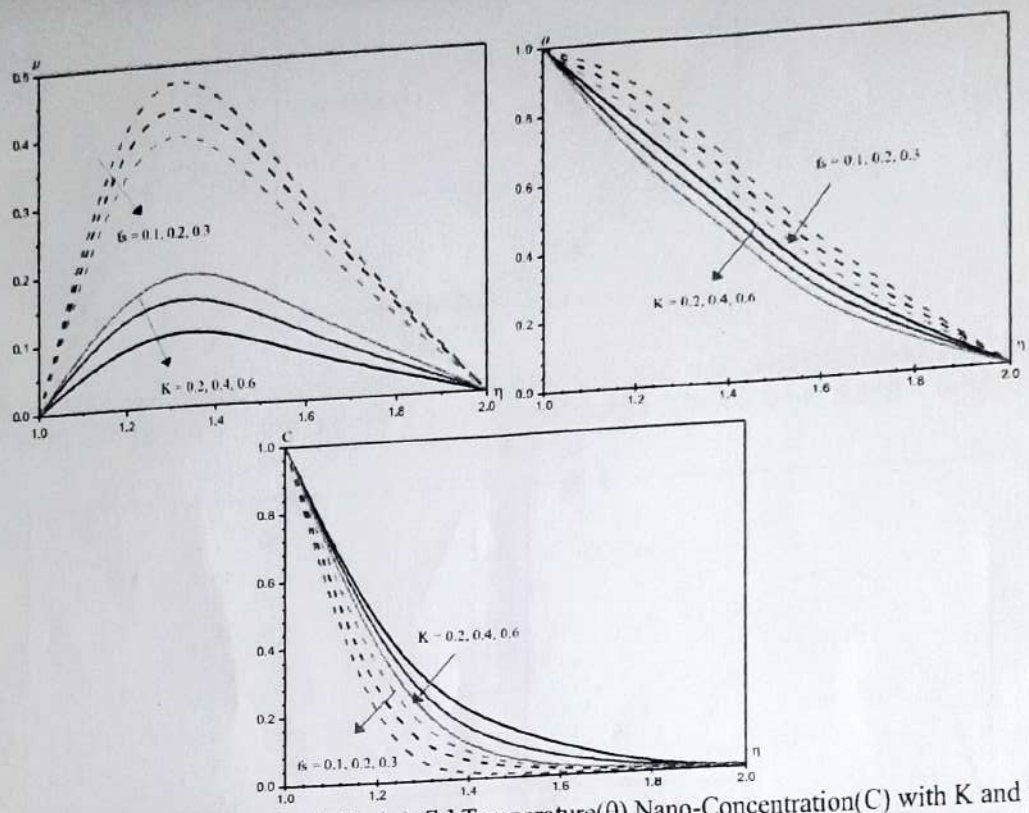

Fig.4 : Variation of [a] axial velocity(w), [b] Temperature(θ),Nano-Concentration(C) with K and fs G=2, M=0.5, B=0.2, Nr=0.5, Nb=0.3, Nt=0.1, E1=0.1, δ=0.2, γ=0.5, Rd=0.5, Q1=0.5, α1=0.1, β1=0.2, Le=1, n = 0.5

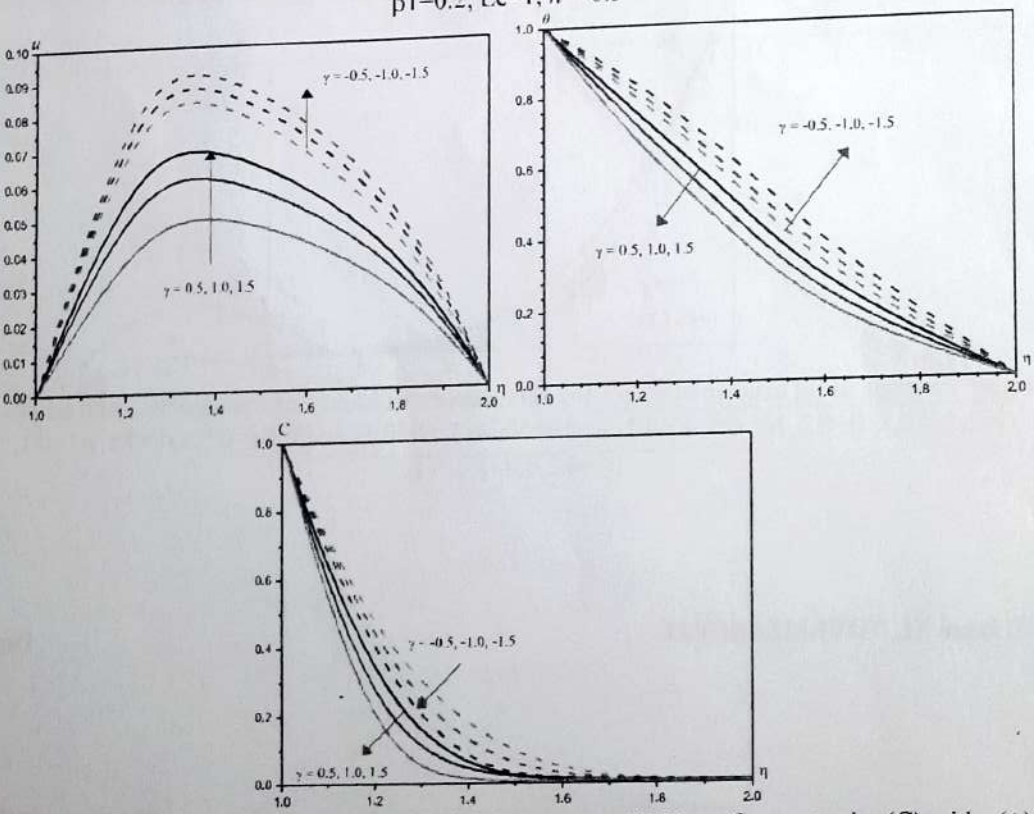

Fig.5 : Variation of [a] axial velocity(w), [b] Temperature(θ),Nano-Concentration(C) with $\gamma(\pm)$ G=2, M=0.5, B=0.2, Nr=0.5, K=0.2, fs=0.1, Nb=0.3, Nt=0.1, E1=0.1, δ=0.2, γ=0.5, Rd=0.5, Q1=0.5, α1=0.1, β1=0.2, Le=1, n = 0.5

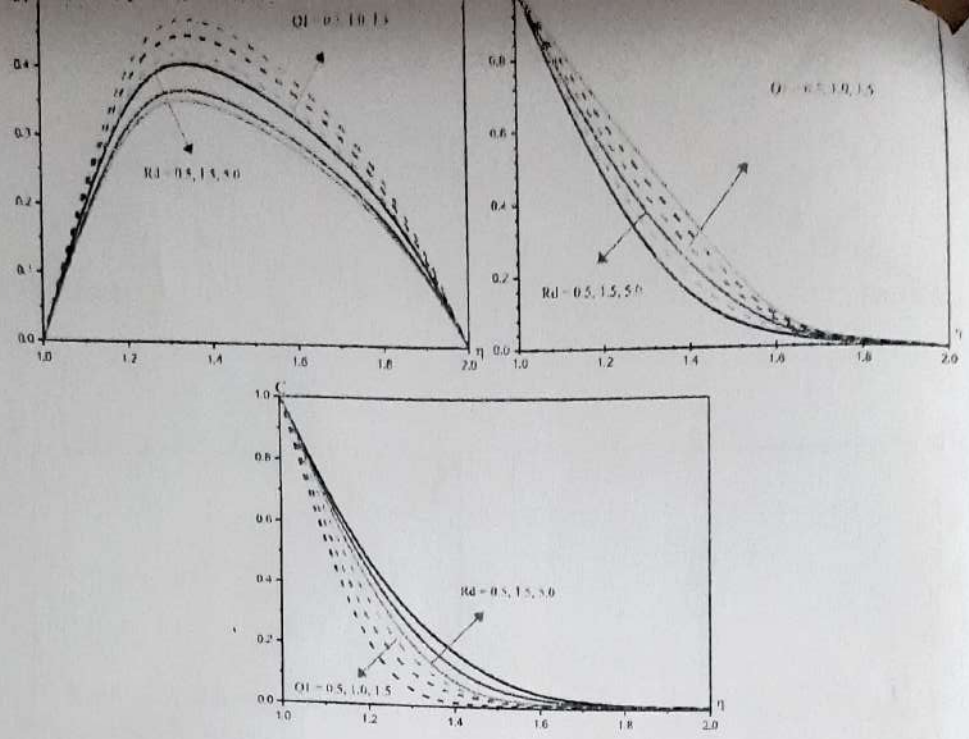

Fig.6 : Variation of [a] axial velocity(w), [b] Temperature(θ),Nano-Concentration(C) with Q1 and Rd G=2, M=0.5, B=0.2, Nr=0.5, K=0.2, fs=0.1, Nb=0.3, Nt=0.1, E1=0.1, δ=0.2, γ=0.5, α1=0.1, β1=0.2, Le=1, n = 0.5

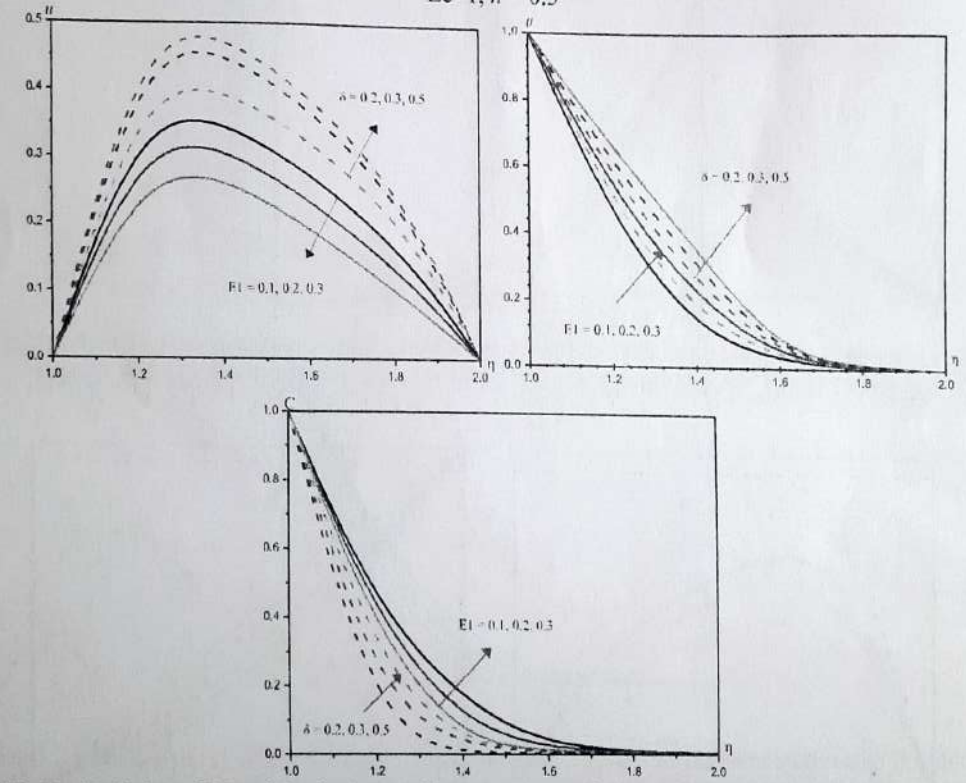

Fig.7 : Variation of [a] axial velocity(w), [b] Temperature(θ).Nano-Concentration(C) with E1 and δ G=2, M=0.5, B=0.2, Nr=0.5, K=0.2, fs=0.1, Nb=0.3, Nt=0.1, γ=0.5, Rd=0.5, Q1=0.5, α1=0.1, β1=0.2, Le=1, n = 0.5

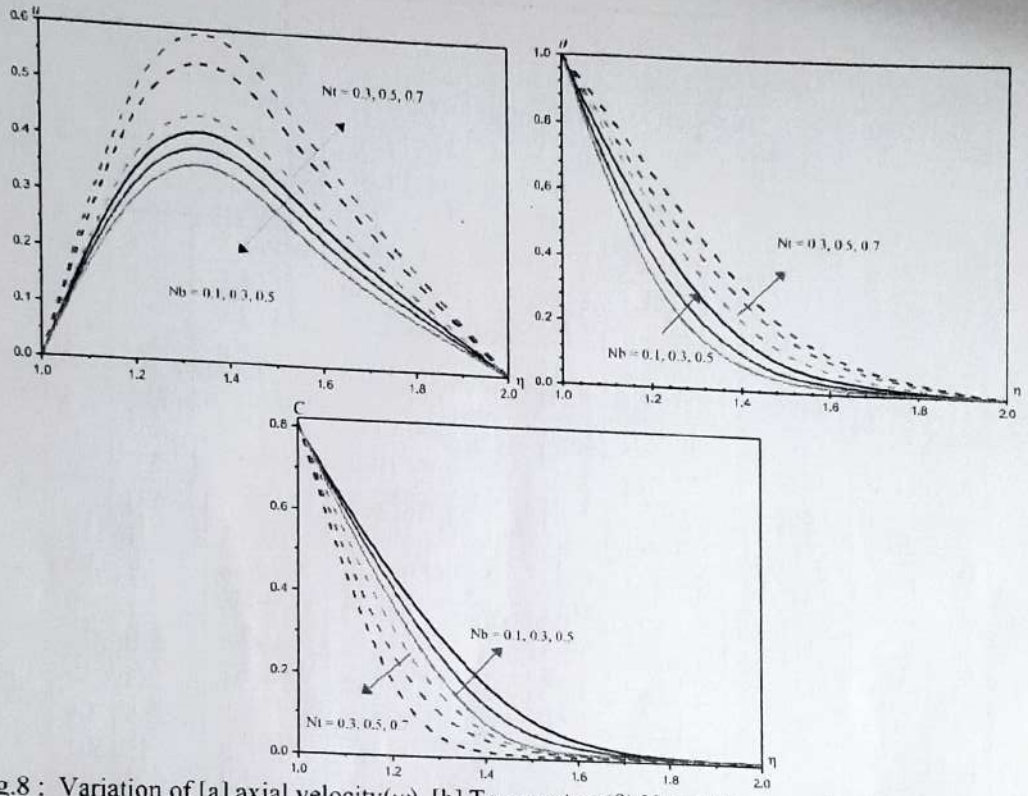

Fig.8 : Variation of [a] axial velocity(w), [b] Temperature(θ),Nano-Concentration(C) with Nb and Nt G=2, M=0.5, B=0.2, Nr=0.5, K=0.2, fs=0.1, E1=0.1, δ=0.2, γ=0.5, Rd=0.5, Q1=0.5, α1=0.1, β1=0.2, Le=1, n = 0.5

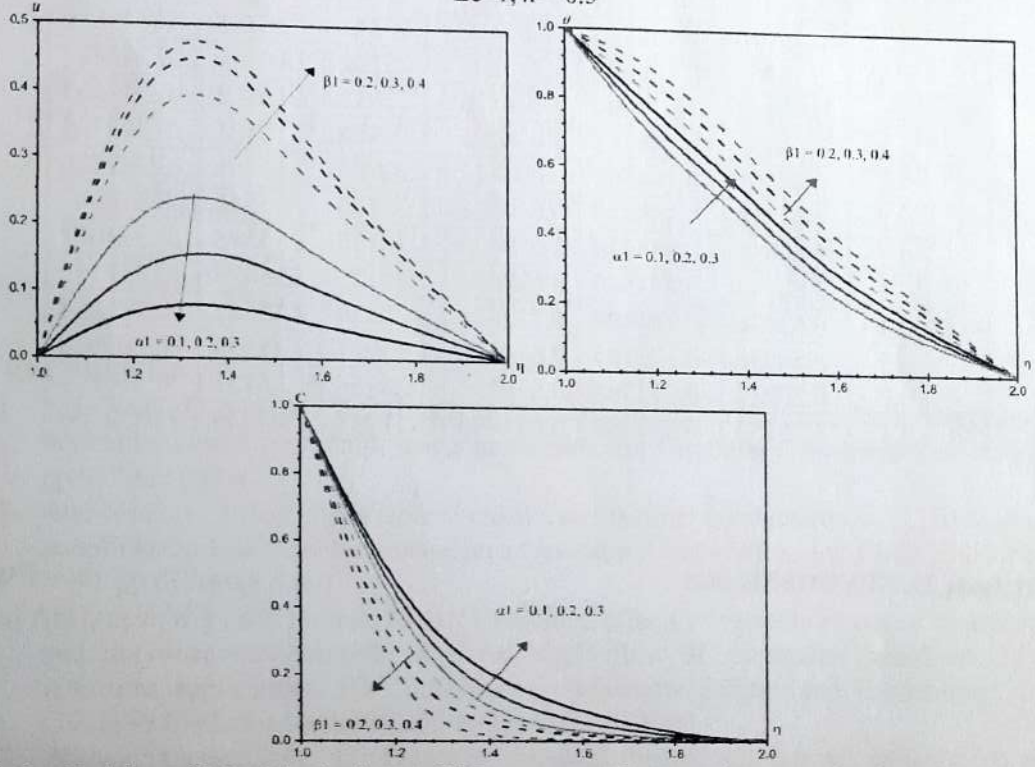

Fig.9 : Variation of [a] axial velocity(w), [b] Temperature(θ),Nano-Concentration(C) with αa and β1 G=2, M=0.5, B=0.2, Nr=0.5, K=0.2, fs=0.1, Nb=0.3, Nt=0.1, E1=0.1, δ=0.2, γ=0.5, Rd=0.5, Q1=0.5, Le=1, n = 0.5

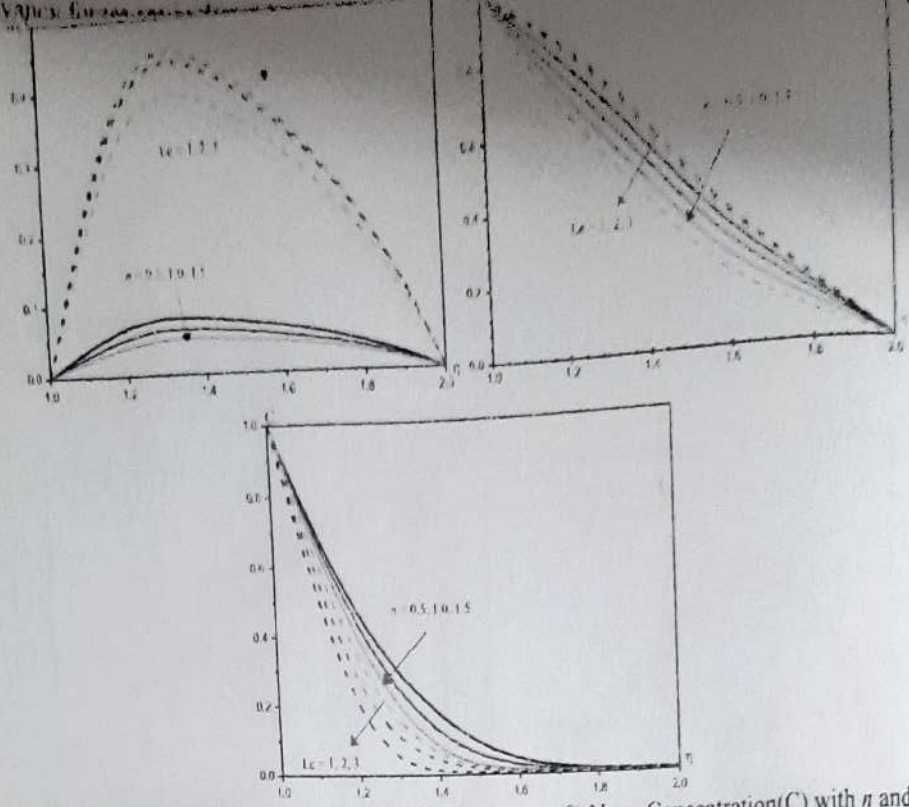

Fig.10 : Variation of [a] axial velocity(w), [b] Temperature(θ),Nano-Concentration(C) with n and Le G=2, M=0.5, B=0.2, Nr=0.5, K=0.2, fs=0.1, Nb=0.3, Nt=0.1, E1=0.1, δ=0.2, γ=0.5, Rd=0.5, Q1=0.5, α1=0.1, β1=0.2

Parameter		Cf(1)	Cf(2)	Nu(1)	Nu(2)	Sh(1)	Sh(2)
G	2	-0.50916	-0.17204	0.674136	1.23911	2.10812	2.10812
	4	1.01891	-0.344464	0.668852	1.24174	2.10645	2.11684
	6	1.52987	-0.517729	0.660008	1.24613	2.12299	2.12299
M	0.5	2.52037	-0.846719	0.709039	1.22614	2.06974	2.06974
	1.0	2.77627	-0.966715	0.409885	1.35588	2.39031	2.39031
	1.5	0.88807	-1.01769	0.27223	1.40968	2.53704	2.53704
B	0.2	2.56617	-0.812163	0.707609	1.22511	2.07113	0.357601
	0.4	2.82197	-0.855005	0.409292	1.35312	2.39076	0.265114
	0.6	2.91609	-0.86463	0.273055	1.40558	2.53598	0.227751
Nr	0.5	0.50916	-0.17204	0.674136	1.23911	2.10812	0.349467
	0.75	0.36919	-0.143656	0.67486	1.23881	2.10711	0.349670
	1.00	0.25701	-0.120882	0.675297	1.23862	2.10691	0.349827
K	0.2	0.50916	-0.17204	0.674136	1.23911	2.10812	0.349467
	0.4	0.50059	-0.168215	0.674206	1.23908	2.10801	0.349752
	0.6	0.49235	-0.164565	0.67427	1.23904	2.10798	0.349526
fs	0.1	2.61715	-0.888679	0.629062	1.26155	2.15555	0.330907
	0.2	2.60855	-0.885319	0.629436	1.26135	2.15515	0.331072
	0.3	2.60445	-0.883544	0.629633	1.26125	2.15495	0.331159
Nb	0.3	0.52936	-0.181109	0.712678	1.20339	2.47547	0.171644
	0.5	0.50936	-0.172107	0.674136	1.23911	2.28159	0.281628
	0.7	0.50727	-0.171768	0.630191	1.28156	1.98121	0.410879
Nt	0.1	2.75752	-0.971197	0.641405	1.31839	2.44936	0.0832746

Parameter		Cf(1)	Cf(2)	Nu(1)	Nu(2)	Sh(1)	Sh(2)
	0.3	3.20349	-1.18674	0.361976	1.46826	3.43945	-0.371341
	0.5	3.45645	-1.30879	0.263731	1.52086	4.22079	-0.757245
E1	0.1	0.50916	-0.17204	0.674136	1.23911	2.10812	0.349467
	0.2	0.50804	-0.17159	0.673952	1.23973	2.09128	0.350521
	0.3	0.50698	-0.171174	0.673804	1.24022	2.06349	0.359904
δ	0.2	2.54969	-0.856445	0.707119	1.22576	2.09692	0.352504
	0.3	2.80583	-0.976198	0.409934	1.35358	2.43713	0.256323
	0.5	2.91247	-1.02518	0.274553	1.40585	2.59649	0.216518
γ	0.5	0.50916	-0.17204	0.674136	1.23911	2.10812	0.349467
	1.0	0.51296	-0.173497	0.674642	1.23745	2.14744	0.349471
	1.5	0.51296	-0.173497	0.674642	1.23745	2.17761	0.334127
	-0.5	2.44566	-0.814498	0.713567	1.2279	1.74151	0.438588
	-1.0	2.71779	-0.945226	0.393171	1.37605	2.03068	0.338705
	-1.5	2.81013	-0.992337	0.236591	1.44852	2.05033	0.320522
Rd	0.5	2.56006	-0.869339	0.631268	1.26042	2.15322	0.331841
	1.5	2.38815	-0.777763	0.794341	1.1379	2.10572	0.331835
	5.0	2.32145	-0.742885	0.857304	1.09378	1.90574	0.463209
Q1	0.5	2.62497	-0.899949	0.555516	1.29378	2.23447	0.307616
	1.0	2.74141	-0.954717	0.410609	1.3545	2.38947	0.26377
	1.5	2.84487	-1.00293	0.273536	1.4083	2.53561	0.225188
α1	0.1	0.65794	-0.199739	0.673021	1.23973	2.09892	0.350815
	0.2	0.65715	-0.199596	0.673019	1.23973	2.09894	0.350817
	0.3	0.65612	-0.199374	0.673018	1.23972	2.09896	0.350822
β1	0.2	3.42102	-1.04466	0.599274	1.27335	2.1867	0.321358
	0.3	3.42507	-1.04538	0.598838	1.27342	0.18715	0.32131
	0.5	3.43555	-1.04751	0.597776	1.27357	2.18824	0.32122
n	0.5	0.50869	-0.171873	0.674066	1.23932	2.09783	0.351146
	1.0	0.50936	-0.172107	0.674136	1.23911	2.10464	0.349921
	1.5	0.50985	-0.17228	0.674208	1.2389	2.1188	0.347728
Le	1	2.73529	-0.937264	0.627651	1.2528	2.59032	0.207777
	2	2.84591	-0.978889	0.626239	1.24549	3.04534	0.11933
	3	2.94475	-1.01284	0.625043	1.23936	3.51557	0.0576512

8. REFERENCES

[1]. Abu-Nada, E., Masoud, Z., Hijazi, A: Natural convection heat transfer enhancement in horizontal concentric annuli using nanofluids, Int Commun Heat Mass Transf, V.35, pp.657-665(2008).

[2]. Abu-Nada, E: Effect of variable viscosity and thermal conductivity of Al_2O_3-water nanofluid on heat transfer enhancement in natural convection, Int J heat Fluid Flow, V.30, pp.679-690(2009).

[2a] Abou-zeid M.Y. and Ibrahim M.G. : Combined effects of variable electrical conductivity and microstructural/multiple slips on MHD flow of micropolar nanofluid : Food industries applications. IOP Conf.Series : Materials Science and Engineering: 1130 (2021) 012049, doi.10 1088/1757-899f/1130/1/012049

[3]. Alivene, B., Sreevani, M: Effect of thermo-diffusion and thermal radiation on non-Darcy convective heat and mass transfer flow in a cylindrical annulus with chemical reaction, International Journal of Mathematical Archive-8(1), 34-42(2017).

exponentially stretching sheet embedded in a thermally stratified medium with exponentially heat generation. J of Heat and Mass tran Res. V.2:pp.63-78(2015).
[5]. Bandita P. E_ects of variable viscosity and thermal conductivity on the unsteady two slip flow of micropolar fluid over a vertical plate. Intern J of Comp Appl Tech and Res. V.6(7):pp.293-298(2017).
[6]. Choi, S.U.S: Enhancing thermal conductivity of fluid with nanoparticles, developments and applications of non-Newtonian flow. ASME FED 231, pp.99-105(1995).
[7]. Devi SPA, Prakash M. Temperature-dependent viscosity and thermal conductivity e_ects on hydromagnetic flow over a slendering stretching sheet. J of Nig Math Soc. pp.34:318-330(2015).
[8]. Dulal P, Hiranmony M. E_ects of temperature-dependent viscosity and variable thermal conductivity on mhd non-Darcy mixed convective di_usion of species over a stretching sheet. J of Egy Math Soc.V.22:pp.123-133(2014).
[8a]. Gayathri, P : Impact of Variable Viscosity, Activation Energy on MHD Mixed Convective Heat and Mass Transfer Flow of a Nanofluid in a Cylindrical Annulus, *YMER* : Vol.21. Issue:4, PP:211-223, April-2022, ISSN : 0044-0477, www.ymerdigital.com
[9]. Gireesha B.J., M. Archana, B. Mahanthesh, Prasannakumara B.C., "Exploration of activationenergy and binary chemical reaction effects on nano Casson fluid flow with thermal and exponentialspace-based heat source", Multidiscipline Modeling in Materials and Structures, V.15 : 1, pp.227-245, (2019)
[10]. Gopal CH, Jadav K. E_ects of variable viscosity and thermal conductivity on magnetohydrodynamics free convection dusty uid along a vertical porous plate with heat generation. Tur J of Phy. pp.40:52(2016)
[11]. Ijaj Khan M, Sohail A, Khan, Hayat T, Imran Khan M and Alsaedi A : Arrchenius activation energy impact in binary chemically reactive flow of TiO_2-Cu-H2O hybird nanomaterial, International Journal of Chemical Reactor Engineering, (2018), DOI:10.1515/ijcre-2018-0183
[12]. Isaac LA, Anselm OO. E_ects of variable viscosity, dufour, soret and thermal conductivity on free convective heat and mass transfer of non-Darcian flow past porous at surface. Amer J of Comp Math ,pp.357-365(2014).
[13]. Jadav K, Hazarika GC. E_ects of variable viscosity and thermal conductivity on mhd free convection flow of dusty fluid along a vertical stretching sheet with heat generation. Intern Res J of Eng and Tech. V.3(2):pp.1029-1038(2016).
[14]. Kareem RA, Salawu SO. Variable viscosity and thermal conductivity e_ects of soret and dufour on inclined magnetic _eld in non-Darcy permeable medium with dissipation. Brit J of Math and Comp Sci. 22(3):pp.1-12(2017).
[15]. Khan M.I.T, Hayat M, Khan I, and Alsaedi A: Activatio Energy impact in Nonlinear Radiative Stagnation Point Flow of Cross Nanofluid, Int.Communiations Heat Massachusetts Transfer, V.91, pp.216-224, (2018)
[16]. Madhusudhana Reddy, Y., Rama Krishna, G.N. and Prasada Rao, D.R.V: Numerical study of Convective Flow of CuO-water and Al_2O_3-water nanofluids in cylindrical annulus, Int. Journal of Research & Development in Tech., Vol. 7, Issue 3,pp. 142-148 (2017).
[17]. Makinde O.D., Mabood F, Khan W.A., Tshehla M.S. : MHD flow of a variable viscosity nanofluid over a radially stretching convective surface with radiative heat, Journal of Molecular Liquids, V.219, pp.624-630, (2016), www.elsevier.com/locate/molliq, http://dx.doi.org/10.1016/j.molliq.2016.03.078

ISSN NO : 2347-3150

[18]. Mallikarjuna, B, Ali J Chamkha and Bhuvana Vijaya, R: Soret and Dufour effects on double diffusive convective flow through a non-Darcy porous medium in a cylindrical annular region in the presence of heat sources., J. Porous Media,V.17(7),pp. 623-636(2014).

[19]. Mokhtari Moghari, R., Akbarinia, A., Shariat, M., Talebi, F., Laur, R: Two phase mixed convection Al_2O_3-water nanofluid flow in an annulus, Int J Multiph Flow, V. 37(6), pp.585-595(2011).

[20]. Nagasasikala, M and Phrabhakar Rao G: Heat and mass transfer of a MHD flow of a nanofluid through a porous medium in an annular, circular region with outer cylinder maintained at constant heat flux, Presented in NCIT Conference, SSBN Degree College, Ananatapuramu (2016).

[21]. Parvin, S., Nasrin, R., Alim, M.A., Hossain, N.F., Chamka, A. J: Thermal conductivity variation on natural convection flow of water-alumina nanofluid in an annulus, Int J Heat Mass Transf, V.55 (19-20),pp.5268-5274(2012).

[22]. Putra, N., Roetzel W, Das, S.K: Natural convection of nanofluids, Heat and Mass Transfer, V.39 (8-9),pp.775-784(2003).

[23]. Ramakrishna G.N. and Prasada Rao D.R.V., Impact of soret effect, radiation absorption on hydro-magnetic convective heat and mass transfer flow of a nanofluid in a cylindrical annulus with chemical reaction and irregular heat sources, AEGAEUM JOURNAL, Volume 9, Issue 9, 2021, Page No:30-46, ISSN: 0776-3808, http://acgaeum.com

[24]. Saida Rashid, Tasawar Hayat, Sumaira Qayyum, Muhammad Ayub, Ahmed Alsaedi, "Threedimensionalrotating Darcy–Forchheimer flow with activation energy", Int. Journal of Numerical Methods for Heat & Fluid Flow, 29 : 3, pp.935-948, (2019)

[25]. Sandhya G, Sreelakshmi K, Sarojamma G, : Effect of Arrhenius activation energy and dual stratifications on the MHD flow of a Maxwell nanofluid with viscous heating, The International Journal of Engineering and Science (IJES), ISSN (e): 2319 – 1813 ISSN (p): 23-19 – 1805, pp.55-60, (2020)

[26]. Shivakumara, I.S., Prasanna, B.M.R., Rudraiah, N., and Venkatachalappa, M: Numerical study of natural convection in a vertical cylindrical annulus using a non-Darcy equation, Journal of Porous Media, 5 (2). Pp.87-102(2002).

[27]. Singh V, Shweta A. Flow and heat transfer of maxwell fluid with variable viscosity and thermal conductivity over an exponentially stretching sheet. Amer J of Fluid Dyn.V.3(4):pp.87-95(2013).

[28]. Soleimani, S.I., Sheikholeslami, M., Ganji, D.D., Gorji-Bandpay, M: Natural convection heat transfer in a nanofluid filled semi annulus enclosure, Int Commun Heat Mass Transf, V.39 (4), pp.565-574(2012).

[29]. Sree Devi, G., Raghavendra Rao, R., Chamka, A.J and Prasada Rao, D.R.V: Mixed convective heat and mass transfer flow of nanofluids in concentric annulus with constant heat flux, Procedia Engineering, V.127, pp.1048-1055(2015).

[30]. Srinivas, G., Srikanth Gorti, V.P.N., Suresh Babu, B and Sreenatha Reddy, S: Particle spacing and chemical reaction effects on convective heat transfer through a nanofluid in cylindrical annulus, Procedia Engineering, 127,pp.263-270 (2015).

[31]. Sudhakara Reddy, Convective Heat and Mass Transfer Flow of Nanofluid in Channels/Ducts, Ph.D. thesis submitted to Sri Krishnadevaraya University, Ananthapuramu, A.P., India, 2019

[32]. Sudarsana Reddy, P., Chamka, A.J: Soret and Dufour effects on MHD convective flow of Al2O3-water and TiO2- water nanofluids past a stretching sheet in porous media with heat generation/absorption., J. Advanced Powder Technology, V. 27, pp.1207-

Heat and Mass Transfer Flow of Nanofluids in a Circular Annulus, *International Journal of Mathematical Archive (IJMA)*, Issue 6, Vol. 8, pp 53-62 , ISSN 2229-5046(2017).
[34]. Tao, L.N: On combined and forced convection in channels, ASME J. Heat Transfer, V.82, 233-238(1960)
[35]. Tayappa, H. and Sulochana, C. Non-Darcy Convective Heat and Mass Transfer Flow in a Circular Annulus with Soret, Dufour Effects and Constant Heat Flux. International Journal of Scientific and Innovative Mathematical Research (IJSIMR) V. 2, Issue 8, August, pp 684-697(2014).
[36]. Vajravelu K, Prasad KV, Chiu-on N. Unsteady convective boundary layer flow of a viscous fluid at a vertical surface with variable fluid properties. Nonl Analy: Real World Appl.;V.14:pp.455-464(2013)
[37]. Wen, D and Ding, Y: Formulation of nanofluids for natural convective heat transfer applications, Int J Heat Fluid Flow, V. 26(6),pp. 855-864(2005).
[38]. Zeeshan A., Shehzad N., Ellahi R., "Analysis of activation energy in Couette-Poiseuille flow of nanofluid in the presence of chemical reaction and convective boundary conditions", Results in Physics,V.8 ,pp. 502–512(2018).